HEFAT2008
6th International Conference on Heat Transfer, Fluid Mechanics and Thermodynamics
30 June to 2 July 2008
Pretoria, South Africa
Paper number: K5

RECENT PROGRESS ON THE INVESTIGATION OF PHASE CHANGE AND INTERFACIAL CONDITIONS IN MICROSYSTEMS

Sefiane K.*
*Author for correspondence
School of Engineering&Electronics,
University of Edinburgh,
Edinburgh, EH9 3JL,
UK,
E-mail: k.sefiane @ed.ac.uk

ABSTRACT

Evaporation of liquids is a fundamental phenomenon pertaining to a wide range of industrial and biological processes. In this paper we present recent results on evaporation of liquids and interfacial phenomena in the case of two configurations: menisci in micro-channels and sessile wetting droplets . Interfacial temperature is a key factor in the phase change process. The access to the interface temperature at the micro-scale has been a challenging task. Recently Ward and Duan [22] have investigated the cooling effect resulting from the evaporation of water in a reduced pressure environment by using micro-thermocouples near the interface. They show an increase in the cooling effect with the increase in the evaporation mass flux. They also show an important experimental result that is in contrast with classical kinetic theory and non-equilibrium thermodynamics. The temperature in the vapour phase is higher than in the liquid phase. The authors also discussed the fundamental question about the interfacial conditions during phase change. Indeed, as instrumentation has developed, it has become possible to make measurements of the temperature within one-mean-free path of the interface of water as it evaporates steadily, and these measurements have not supported the prediction from classical kinetic theory that the interfacial vapour temperature less than the interfacial liquid temperature. In a first part of the paper, we present data from an experimental study that has been performed to investigate the evaporation of a liquid in a capillary microchannel. The phase change has been found to induce convection patterns in the liquid phase below the meniscus interface. The liquid convective structure has been revealed using μ-PIV technique. When extra heating is supplied to the system, the convection pattern is altered and eventually reversed depending on the relative position of the heating element with respect to the liquid-vapour interface. An IR thermography is used to measure temperature gradients generated by the heater along the capillary wall and of the interface. This allowed us to investigate the relation between the temperature gradients applied along the wall and the convection taking place in the liquid under the thermocapillary stress hence generated.

In the second part of the paper we investigate the complexity of the evaporative process of wetting drops by means of IR thermography. The obtained data for volatile sessile drops clearly show that there are phenomena at work which, whilst invisible to the naked eye, may have a great importance in many evaporation dependent areas. The naturally occurring thermal instabilities (wave like thermal fluctuations) shown by many investigated working fluids are clearly distinct from each other, and can also be manipulated by altering the evaporation parameters such as substrate material and substrate temperature. What is also interesting to note is that whilst these waves have been observed for these relatively volatile liquids, there appears to be no such behaviour in pure water droplets. The visual observations presented in this paper form the basis for which a full systematic analysis of the wave behaviour can be achieved. Wave number, frequency, velocity, and amplitude are all parameter which can be measured and then used to characterise the behaviour of each fluid. The above described phenomena are entirely self-generated by the phase change process.

INTRODUCTION

Over the last century surface tension driven phenomena have attracted much attention due to the recognition that surface tension becomes an important parameter in small scale processes [1-5]. Many industrial applications such as crystal growth, glass manufacture, surface acting agents, combustion,

evaporation and condensation of thin liquid films rely on the effect of surface tension. Many arising problems in these processes have only been solved for very simple cases and even then in quite a qualitative manner. Experimental difficulties in making small scale measurement of parameters such as temperature, pressure and velocity, limit a full understanding of the phenomena. In particular evaporation of liquids is used in heavily thermally loaded applications. Cooling technologies are needed for dissipating high heat fluxes in applications such as x-ray medical devices, high-power lasers, and fusion reactors. Heat loads for fusion reactor components require cooling schemes that could dissipate heat fluxes of the order of $104W/cm^2$. The need to handle high heat fluxes in industry and various engineering fields (refrigeration applications, food processing) has led to the development of new heat and mass transfer equipment. Such equipment include conventional heat pipes, which rely on the vaporisation of a fluid in a porous media and the use of compact and plate heat exchangers. Other new equipment such as capillary pumped loops and loop heat pipes have been recently developed. Flowing liquid films are used in a large number of heat and mass transfer applications including falling-film evaporators, film cooling of rocket nozzles and turbine blades, nuclear reactors cooling, packed columns, vertical condensers, and wetted-wall columns. High transfer coefficients are the main incentive for using thin liquid films. However, the surface of the film is susceptible to disruption by a number of phenomena such as gas-flow shear, evaporation, boiling, and thermocapillary effects. Through the loss of transfer area, any of these mechanisms can, at best, reduce overall transfer rates and at worst lead to equipment damage. The use of equipment such as heat pipes and compact heat exchangers revealed major performance anomalies [6],[7]:

- Start-up failures with no explanation;
- Pressure oscillations;
- Unstable system operation in evaporating devices.

These types of anomalies are well known in the industry using heat transfer devices. However, the existing design models do not give any physical explanation. The relationship between the observed anomalies and the evaporation process in the devices is not well understood. Over the last decades, there has been continued interest in the study of the above processes. It is worth noticing that some parameters that were not amenable to experimental control and/or measurement were often neglected in the design. Wetting effects and evaporating hydrodynamic and thermal instabilities occurrence fall under this category. In the recent years many researchers [8-11] have performed fundamental studies on the stability of an evaporating meniscus. The configuration studied is a meniscus wetting a wall along which a temperature gradient is imposed by the heat source. Pratt et al. [12] have investigated the stability of a volatile pentane meniscus in a tube where a heat source is applied at the edge of the tube. They have demonstrated that the thermocapillary stress arising from the applied temperature gradient can lead to the meniscus receding, but did not investigate the hydrodynamics within the liquid phase and the role of such temperature gradients on this flow. Based on these studies, and based on our previous investigation [13-14] in this field it has been demonstrated that the triple line region plays a determining role in the above processes; indeed wetting effects recently emerged into consideration. It has been well demonstrated that the critical heat flux mechanism depends on the instabilities occurring at the contact regions between liquid-solid and vapour. The evaporating menisci at the bottom of vapour mushrooms near the CHF region and the conditions of the instability are determining factors; investigating those conditions will contribute to the improvement of boiling heat transfer. The experimental determination of both matter and heat fluxes at evaporating surfaces and the determination of the surface instability thresholds need new experiments to be designed. These fundamental aspects are of great interest for practical applications. Thermocapillary stresses associated with these problems lead to thermocapilalry driven flows within the bulk of the liquid. From a fundamental point of view, fluid motion driven by a temperature gradient imposed along a free liquid-gas interface is a well documented phenomenon (Thermocapillary convection), [15]. Smith and Davis, (1983), [16] studied the stability of an infinite fluid layer with a free surface subjected to a temperature gradient along the interface. This pioneering work revealed the oscillatory nature of the instability when in super critical conditions. The 3D, time depended linear stability analysis of Smith and Davis (1983) and Smith (1986), [17] predicted the occurrence of what is called Hydrothermal waves (HTW). Hydrothermal waves have been subsequently confirmed by many experimental investigations studying shallow rectangular pools of liquids, [18]-[19]. Hydrothermal waves seem to appear for shallow fluids and small temperature gradients. They propagate from the cold side to the hot one and the wave vector can make an angle to the temperature gradient depending on the Prandtl number, of the liquid. For small Pr numbers HTW propagate parallel to the temperature gradient. For large Pr numbers, they travel almost perpendicular to the temperature gradient, [20]. HTW have also been investigated in annular geometries, where a temperature gradient is imposed between the centre and the outer wall. Recently N. Garnier and Chiffaudel (2001) investigated HTW in thin annular pools of silicon oils, a temperature gradient between a cold centre and a hot outer wall were studied. The authors reported HTW with spiral – like arms circling the annulus. For smaller fluid depths (less than the capillary length), the observed HTW propagate radially from the centre to the outer edge, a stability diagram for HTW was also reported. Depending on the critical value of the ΔT and the fluid depth, stability regions could be distinguished. Schwabe et al. (2003), [21] reported temperature fluctuations associated with HTW's propagating in an annulus. The temperature oscillation amplitude and frequency is found to depend on the imposed temperature gradient as well as the fluid depth.

In all above investigations, evaporation and its contribution to the generation of HTW has not been studied. Interfacial temperature is a key factor in the phase change process. Ward and Duan (2004), [22] have investigated the cooling effect resulting from the evaporation of water in a reduced pressure environment. They showed substantial temperature drops due to evaporative cooling effect which increases with the increase in the evaporation mass flux.

Spontaneous evaporation of sessile drops is a phenomenon encountered in everyday's life experience as well as a wide range of biological and engineering areas. During the spontaneous evaporation of sessile drops, the latent energy required for evaporation leads to a liquid temperature drop which depends on the volatility of the liquid and the thermal properties of the substrate. Volatile sessile droplets can exhibit temperature gradients arising from non-uniform evaporation along the liquid-vapour surface, [23]. These temperature gradients are self generated and evolve during the lifetime of evaporating drops. They can lead to a range of thermocapillary effects like Marangoni convection within the drops, [24]. Despite numerous studies much is still unknown about the physical behaviour of evaporating droplets. Factors that influence the evaporation behaviour, such as surface tension, temperature effects, liquid viscosity, density, vapour phase temperature and also thermal convection inside the liquid make obtaining a full understanding of the process difficult. In the following section we will present the findings of two experimental investigation, evaporation of menisci in capillaries and evaporation of wetting sessile drops. These two cases present different geometries but the fundamental physical phenomena are very similar.

EXPERIMENTAL PROCEDURES AND RESULTS

Evaporation in capillaries

A capillary tube of 600 μm has been vertically plunged in a pool of ethanol or methanol and the liquid has been allowed to rise inside the tube above the pool level because of the capillary forces action and a meniscus curved interface is formed. The liquid is allowed to evaporate in the open environment surrounding the tube at 1 atm and room temperature of 25 °C. Two experimental studies were carried out independently in order to map: the liquid flow field in the capillary and the temperature field of the tube wall and of the liquid-vapour interface. A high speed camera is attached to a microscope, a PC with dedicated software for acquisition and storing is employed and a laser to illuminate the fluid is used. The high speed camera is a Phantom v.4.3 model with a CCD array of 512x512 pixels and a frame rate at full array of 1,000 frames per second. Because of the laser-microscope-tube specimen spatial arrangement, a mirror is used to divert the laser beam along the vertical capillary tube. The microscope is necessary because of the small tube size considered. The flow pattern is unveiled by the use of micro-Particle Image Velocimetry (μ-PIV). This technique consists in seeding the fluid with particles of the right size and density that scatter the light produced by a coherent light source (laser). Two image of the scattered light are recorded on the CCD camera and computer correlated in order to obtain the velocity vector map. μ-PIV technique is substantially different from standard PIV. In standard PIV [25], a laser sheet created by means of mirrors and lenses is focused in the camera's depth of focus. In μ-PIV [26-28] a microscope has to be used because of the small sizes involved. It becomes almost impossible to focus the laser sheet on the microscope depth of focus. Therefore, a different strategy is employed. The laser beam is directed on the entire flow and the duty to create an optical sheet is left to the microscope narrow depth of focus. Many issues arise in this case as described in [26-28]. The way we solved these issues for the present experimental setup has been described in details in Buffone et al. [29]. We report here only the main features: in the cross-correlation technique employed using borosilicate spherical glass particles (Ø = 3 μm, ρ= 1.1 g/cm^3) with an interrogation window of 8x8 pixels and an overlap of 50%, 16,129 vectors were extracted reaching a vector spatial resolution of 0.64 μm.

The optical distortion encountered by looking through a round tube has been corrected a posteriori as also outlined in Buffone et al. [29]. This has lead to diametrical sections of the tube smaller than the tube internal diameter, because close to the tube edge there is internal total reflection.

An electric heater has been built, on the external surface of the capillary tube by depositing a silver coating with the use of an air brush. The thickness of the paint is enough to ensure a dissipation of up to 2 W. This power is measured by the use of a voltmeter and ammeter provided with the power supply. Moving the capillary tube with respect to the pool, the meniscus inside the tube was put in the wanted position with respect to the electric heater. Two positions were investigated in this study. The meniscus has been positioned just below the heater (namely: heater in the vapour side) and at the capillary top (namely: heater in the liquid side). The heater power delivered was varied in steps in the range of 0.02 – 2 W; after each run the heater was shut down allowing the meniscus to rewet the tube before another power was selected. A lower upper limit is reached with the heater in the liquid side, because of the boiling limit reached in the micro-channel. With the heater in the liquid side, the meniscus remains stuck at the capillary edge no matter which power is applied as far as no boiling is set in. When the heater is in the vapour side, the meniscus is no longer anchored to the tube edge and small heater power suffices to put it in motion. We have demonstrated, [30], for the case of the heater in the vapour side that the liquid vettability is increased (apparent contact angle decreases) as the heater power increases; this because of the thermocapillary stress arising at the meniscus triple line. When applying power, the forces balance at the triple line is altered and the meniscus moves down along the tube where a new equilibrium can be found. Because of the meniscus motion, it becomes more difficult to compare the results of μ-PIV on convection strength with different powers applied when the heater is on the vapour side. Fortunately the time scale of the meniscus motion is larger (essentially because of viscous forces at the triple line) than the convection time scale and a comparison based on the convection strength is thus possible. We have therefore chosen to compare the μ-PIV results for different heater powers before the meniscus starts to recede, Figure 1.

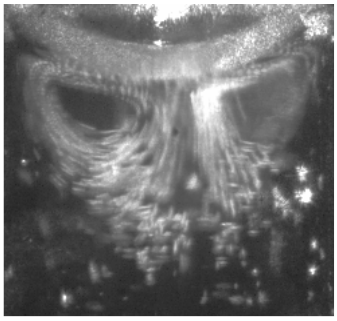

Figure 1 Convection pattern revealed by tracers

For both cases studied (heater in the vapour and in the liquid side) a μ-PIV measurement is taken with the heater off and then compared with the heater on at different powers.

In addition to μ-PIV, infra Red (IR) technique is used to map the temperature distribution along the capillary wall and measure the temperature difference along the meniscus. The IR camera is an Agema 880 model mechanically scanned line by line and cooled at 70 K by liquid nitrogen. The IR detector is a MCT (Mercury, Cadmium and Telluride) based on the SPRITE (Signal Processing in the Element) technology widely used in the top grade military applications. The scanner has two internal blackbody reference sources scanned 2,500 times per second. This leads to an accuracy of ±2 % and a superb sensitivity of 0.07 ˚C at 30 ˚C. The microscope attached to the camera allows for a target size of 1.4x1.4 mm. The camera array is of 140x140 pixels leading to an optical spatial resolution of 10 μm. However, the IR camera works in the long wavelength band of the spectrum (8-12 μm), therefore the spatial resolution expected coincides with this latter physical limit of the camera. A CCD camera is used to first optically focus the specimen with the help of a tiny fiber optics. The shutter mirror then shut this camera, the fiber optics is turned off and the IR scanner is allowed to see the target. A final adjustment is made before any measurement is taken essentially because the optical focus does not exactly coincide with the IR one. A third CCD camera connected to a monitor is used to adjust the meniscus at the wanted position in the tube. A matt black paint is deposited longitudinally on the quarter of the capillary tube pointing on the IR scanner, the other part of the tube being transparent to visualise the meniscus position with the third positioning CCD camera. This black paint is used because from the smooth external tube surface there could be a not negligible reflection and there is a real possibility the IR detector element sees itself. In addition the emissivity of the target can be set with confidence to 0.99 with the paint. Because of the thin black coating (~5-10 μm) with respect to the tube diameter, we can neglect its thermal resistance and assume that the temperature read is the tube one. IR images and movies (at 750 Hz) can be viewed on a monitor where a quick post-processing is possible; storing is also allowed. The images are then transferred to a dedicate PC for full post-processing made with a special in built software (by FLIR Systems).

As far as the experiments on drops are concerned, volatile sessile droplets evaporating on various substrates were investigated using IR thermography. Four liquids (in order of increasing volatility respectively, water, ethanol, methanol and FC72) exhibiting various degrees of volatility were studied. These liquids have Prandtl numbers respectively of, 7, 6.4, 14, and 12.3. Four solids, with different thermal conductivities were used as substrates (in order of increasing conductivity respectively, PTFE, ceramic, titanium and copper). The substrates were coated with a very thin hydrophobic layer to allow for measurable contact angle and give the substrates the same surface energy, making the comparison easier.

The IR camera used is a FLIR ThermaCAM SC3000, it has a thermal sensitivity of 20 mK. The system can acquire images in real time at a rate up to 750Hz. The images acquired are transferred to a dedicated PC with a built in ThermaCAM software. The spatial resolution of the system is of the order of 8 to 9 . In addition to IR thermography measurements, a drop shape analysis goniometer (Kruss DSA100) was used to measure the profile of the drop as it evaporated. This allowed the measurement of the drop profile in time (including, height, angle and base). The investigated drops are pinned to the substrate for most of their lifetime. Hence, the base remains constant while both the height and wetting angle decrease in time.

The experimental setup for the sessile drop investigation, shown in Figure 2, consists of a syringe pump, a horizontal substrate mount, temperature controller, and Infra-Red (IR) analysis equipment. Volatile sessile droplets evaporating on various solid substrates are investigated using IR thermography. We present results for four liquids: water, ethanol, methanol and FC-72. These are chosen to have a range of volatilities and their boiling points are 100°C, 78.3°C, 64.7°C and 56°C, respectively, under atmospheric conditions. Additionally, we use four substrates made of PTFE, Macor (ceramic), titanium and copper, having a range of thermal conductivities 0.25 $Wm^{-1}K^{-1}$, 1.46 Wm^{-1}K-1, 21.9 $Wm^{-1}K^{-1}$ and 401 $Wm^{-1}K^{-1}$, respectively. Care was taken with substrates to ensure homogeneous wettabilities and accurate contact angle measurement; to this end, the substrates were coated with a very thin layer of a fluoropolymer Cytop.

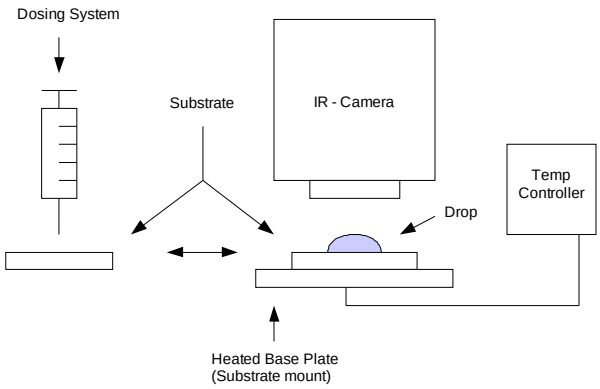

Figure 2 Schematic of the apparatus for studying drops

The drops are deposited using an injection syringe connected to a pump allowing the controlled deposition of drops of known volume onto a solid substrate of chosen

material. To obtain images of the drop behaviour, the IR camera was mounted directly above the substrate, facing vertically downwards onto the evaporating drop. Images are recorded at 50 frames per second using a camera fitted with a microscope lens with a 10×7.5 mm^2 field of view and a minimum focal length of 26mm. The spatial resolution of the system is 8-9 µm.

OBSERVATIONS

Capillaries

Experiments on heated evaporating menisci have been conducted and the flow patterns in the liquid phase below the meniscus interface have been characterized by the use of µ-PIV technique. Two cases have been experimentally analysed.

In the first experiment the heater element has been put in the liquid side of the meniscus whereas for the second one the heater lies in the vapour phase. Experimentally, the case with the heater aligned with the meniscus interface was not tested because the heater is not transparent and therefore no convection pattern can be observed. We have used a 600 µm capillary tube internal diameter filled with ethanol and methanol. Because of the liquids low boiling point, there is a substantial evaporation even without extra heating provided. It has been demonstrated (Buffone et al. [30], [31]) that the convection pattern revealed in this case is mainly due to a non uniform evaporation profile along the meniscus, being larger near the meniscus wedge than at the meniscus centre. This causes a non uniform interfacial thermal field that is basically responsible of the thermocapillary convection observed. Two IR cameras have been employed to map the temperature along the interface and on the tube wall of an evaporating meniscus formed in a confined space, Figure 3. The use of a NDT technique like IR is the only tool available to measure the temperature of a liquid-vapour interface. The good spatial resolution (~30 µm), high sensitivity (20 mK at 30 °C) and great accuracy ±1% of the IR camera used for the interfacial temperature study has allowed to detect the strong evaporative cooling at the meniscus triple line. The liquid evaporates more at the meniscus wedge than in the middle of the capillary. Broadly speaking, convection helps the heat and mass transfer by bringing hot liquid to the colder region; this affects also the driving force that sustains the convection itself. It is shown that this is the case also for the present investigation; the temperature difference is changed by the convection that brings hot liquid into cold regions of the flow. It is also shown that the evaporative cooling effect is stronger at smaller tube sizes and with the use of more volatile liquids. The present experimental evidence supports the hypothesis of a differential evaporative cooling along the meniscus interface responsible for the observed convection. The interfacial temperature for various volatile liquids is shown in Figure 3.

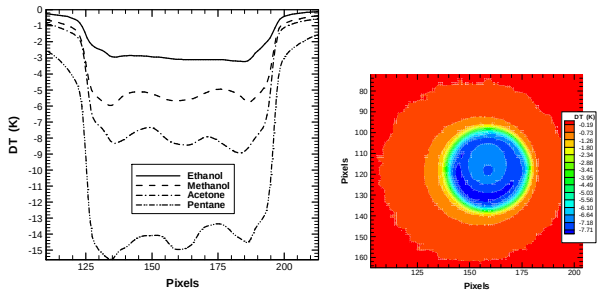

Figure 3 IR picture showing temperature distribution on the surface of four different liquids

The investigation involved the study first of unheated capillary tubes in order to understand the basic mechanisms taking place. Once sufficient information was gathered with the technique, a more complicated situation was studied. The case with heated capillaries is closer to industrial applications such as heat pipes and capillary pumped loops, where a meniscus evaporates in a heated porous wick structure. When the heater is placed below the interface (on the liquid size), it is found that extra-heating (reduces then) enhances the observed convection, Figure 4. Experimental data show that no reversal of the flow can be obtained when the meniscus interface is above the heating element.

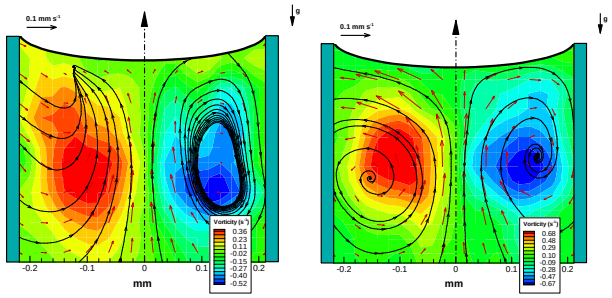

t = 0 heater off t = 4.5 s heater on

Figure 4 PIV sequence for ethanol as liquid and heater (0.3 W) in the meniscus liquid phase.

Figure 4 illustrates the enhancement of convection after applying extra-heating located on the liquid side. The variation of convection strength (vorticity) with the applied heating power is shown in Figure 5. Vorticity seems to decrease in a first stage when power is increased, then increases thereafter. Understanding this trend requires the analysis of the evlution of temperature gradients when power is increased. At lower powers, the vorticity decrease, however this is for a very narrow range of powers.

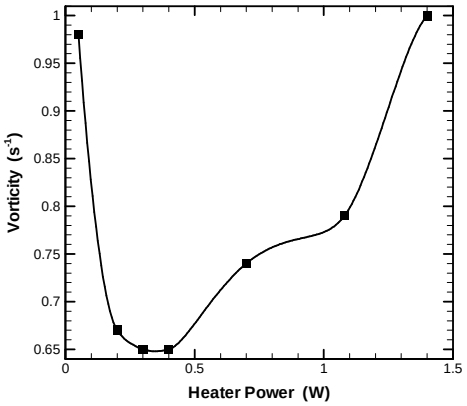

Figure 5 Vorticity as a function of heater power.

In the case the heater is placed on the vapour side and when extra heating is applied, the convection pattern is altered and eventually reversed. This happens when the meniscus lies in the tube below the heating element. Figure 6 illustrates the reversal of the convection when the heater is powered. It is worth mentioning that prior to the reversal of the flow, convection slows down before reversing. This is observed for very low powers. This is an important experimental proof of the fact that the convection under investigation is indeed thermocapillary driven and the temperature profile along the meniscus interface is the key factor.

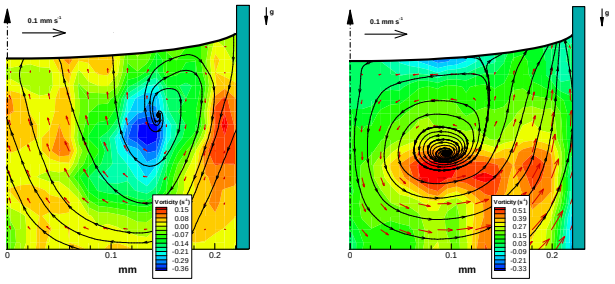

t = 0
heater off

t = 2.5 s
heater on

Figure 6 PIV sequence for methanol as liquid and heater (0.025 W) in the meniscus vapour phase.

The variation of convection strength (vorticity) for the case of the heater in the vapour size with the applied heating power is shown in Figure 7. Temperature gradients along the capillary wall and their variation with the heater power as shown in Figure 8.In the two extreme situations experimentally tested, we have noticed that when the heater is positioned in the meniscus liquid side the convection is influenced but no flow reversal takes place at any heater power; eventually, at high power the liquid starts boiling in the micro-channel.

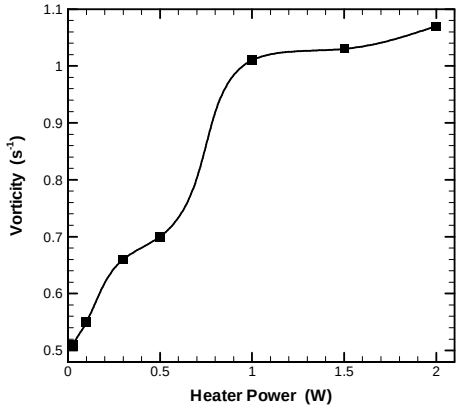

Figure 7 Vorticity vs. heater power for methanol as liquid and heater in the meniscus vapour phase (points are experimental data and line is best fit).

The μ-PIV investigation has proven that the convective patterns in the meniscus liquid phase can be altered and eventually reversed by applying sufficient extra heating, Figure 6.

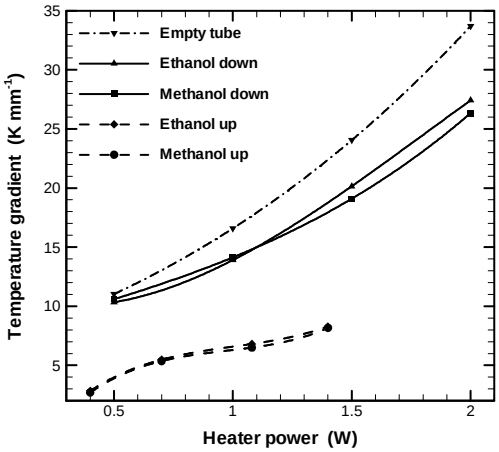

Figure 8 Temperature gradient along the tube wall vs. heater power.

The behaviour of convection described above could be explained with the use of the sketch in Figure 9. With the heater off, the expected temperature at the meniscus wedge (T^-) is lower than that in the centre (T^+). This is the result of evaporative cooling.

When the heater is switched on, more energy is introduced into the system and a different gradient of temperature is created along the tube's walls, but the temperature differences along the meniscus interface is kept. Different scenario takes place with the heater lying in the vapour side (Figure 9).

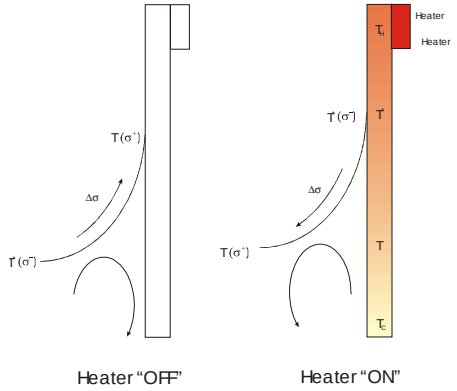

Figure 9 Temperature gradients and convection orientation

Again, when the heater is off the temperature difference is similar to the one in Figure 9 (heater off). However, in this case switching on the heater creates a gradient of temperature along the tube's walls that will affect the temperature profile at the interface. Energy is conducted through the wall material, Figure 8, and an opposite temperature gradient is established along the interface, basically because we can reasonable assume that the temperature at the meniscus centre is similar to the one at the correspondent point on the wall. If the heater power is strong enough the temperature difference along the meniscus interface self-generated because of evaporation is counter balanced by the one imposed by the heater and a net nil gradient is present. So, despite the liquid continues to evaporate, no convection is observed. Increasing further the heater power, the resulting temperature gradient is eventually inverted with the lower temperature now at the meniscus centre. This leads to the convection inversion observed (Figure 6).

Volatile sessile drops

When observing evaporating sessile drops of the four studied liquids, interfacial thermal activity was recorded for methanol, ethanol and FC72. Water did not exhibit any interfacial temperature variations (Figure 10 (a)). Temperature patterns were observed, in the case of methanol and ethanol similar patterns were recorded. Thermal train waves circling the drop surface were clearly visible, Figure 10 (b). In the case of FC72, thermal cells emerging near the drop centre and drifting towards the edge were observed. The cells were larger near the drop apex and smaller near the edge, Figure 10 (c).

The interfacial temperature fluctuations in the case of both Methanol and Ethanol were found to vary by a fraction of a degree, Figure 11. The amplitude of the fluctuation was also found to increase in time. Interfacial temperature fluctuations in the case of both methanol and ethanol drops were of the order of a fraction of a degree, Figure 11.These fluctuations were more pronounced in the case of FC72 drops (~1-2 °K).

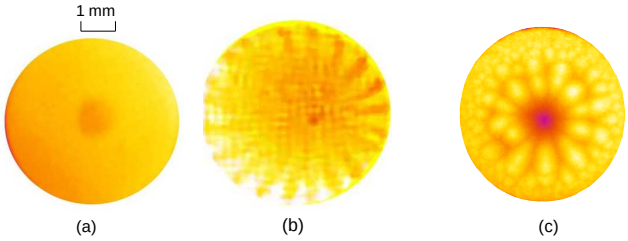

Figure 10 Thermal pattern in evaporating drops, (a) water, (b) methanol and (c) FC72.

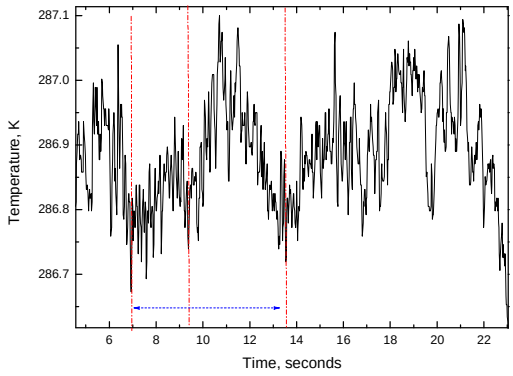

Figure 11 Interfacial temperature fluctuations for a methanol drop.

In the case of ethanol and methanol, the visible waves on the surface of the drop were counted and reported as a function of the dimensionless time, Figure 12. It is clear that as evaporation proceeds, the height decreases in time and the number of visible waves decreases linearly in time. The number of waves is clearly higher for methanol which is more volatile than ethanol.

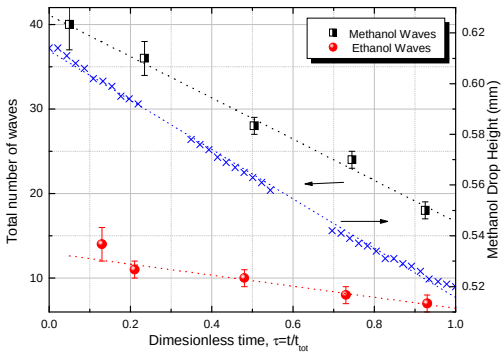

Figure 12 Number of visible waves for methanol and ethanol drops on titanium substrate and drop height evolution.

The use of four different substrates of increasing thermal conductivity allowed us to investigate the role played by the thermal properties of the substrate. For the sake of brevity, the results for two extreme cases (for methanol drops) are presented. As well as the previously noticed trend of decreasing wave number as the evaporation proceeds, the higher conductivity substrate (titanium) exhibits a larger number of waves than the less conductive substrate (ceramic), Figure 13.

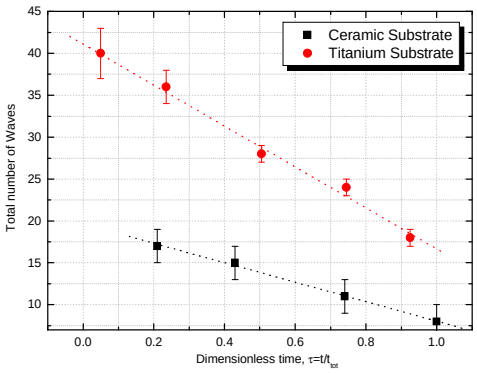

Figure 13 Number of visible waves for methanol drops on ceramic and titanium substrates.

Temperature patterns observed for FC72 were analysed by characterising the size of the cells as a function of the height of the drop. It is clearly found that the size of the cells increases with increasing drop height. The effect of thermal properties of the substrate on the size of observed patterns is inconclusive, Figure 14.

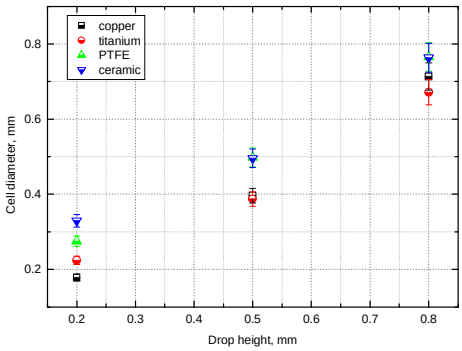

Figure 14 Cells size as a function of drop height for FC72 drops.

Figure 15 shows the evolution of the interfacial thermal patterns for a drop of FC72 throughout its lifetime. The cold spot at the apex of drop is larger and colder at the beginning of the drop lifetime. As the drop evaporates (the height decreases) the intensity of this cold spot and its extent is reduced. This indicates that the overall temperature gradient between the apex of the drop and the edge decreases as the drop evaporates. The size and number of the thermal cells also change as the drop evaporates.

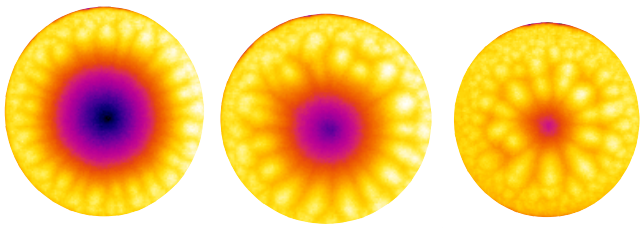

t= 0 t= 2 sec t= 4sec

Figure 15 Evolution of thermal patterns for a FC72 drop in time.

DISCUSSION OF RESULTS FOR DROPS

The thermal patterns observed in the case of Methanol and ethanol drops are consistent with the behaviour observed in the case of HTW as reported in literature. This work is novel in the fact that for the case of an evaporating sessile droplet both the temperature gradient and fluid depth evolve in time. Also, previous work involving HTWs focuses on 2-D annular films with imposed temperature gradients. In our work we consider 3-D liquid drops, the phenomenon occurs spontaneously, and results from evaporation and self-generated gradients. The novelty in the presented results is that both temperature gradient and fluids depth are evolving in time. The phenomenon is also spontaneous, resulting from evaporation and self generated gradients.

The propagation angle of the observed waves has been measured for both ethanol and methanol drops on three different substrates. Methanol exhibits smaller propagation angle than ethanol in all cases. The more conductive substrates show higher propagation angle, Table 1. Methanol and ethanol have Prandtl numbers respectively of 6.5 and 14.2. HTW for liquids with larger Prandtl numbers exhibit higher propagation angle, which is in agreement with our observations. The propagation angles of HTW are found to be higher for liquids with high Prandtl numbers. This result is in agreement with our findings, whereby the Ethanol drops, which have a higher Pr number than Methanol, exhibit larger propagation angles.

Substrate	Liquid	Propagation angle (degree)
PTFE	Methanol	11
	Ethanol	20
Ceramic	Methanol	14
	Ethanol	25
Copper	Methanol	19
	Ethanol	28

Table 1 propagation angle for methanol and ethanol drops on various substrates.

The dependence of the cells on the depth of the liquid observed for the case of FC72 drops (Figure 5) is in good agreement with the observations of Mancini and Maza [32] for evaporating plane liquids. The size of the cells resulting from the evaporation of a liquid is found to decrease as the liquid depth is reduced.

CONCLUSIONS

The present paper summarises the results of two experimental investigations. The first presented study is an experimental study of the hydrodynamics of a meniscus formed by a liquid in capillary tubes undergoing phase change. The non uniform evaporation process along the liquid-vapour interface leads to self-induced temperature field that in turn generates surface tension gradients along the meniscus. The interfacial stress so created drives a vigorous liquid convection that is measured here by the use of a micro-Particle Image

Velocimetry (μ-PIV) technique. Temperature measurements using advanced Infra Red (IR) technique allowed us to measure the interfacial temperature profile and external capillary tube temperature. These two techniques proved to be useful and powerful tools in gathering important and otherwise difficult to monitor information on temperature and velocity fields at the micro-scale. The direction of the self-induced convection can be reversed by applying a temperature gradient along the capillary wall with a heating element. With the tubes vertically plunged in a pool of liquid, it is interesting to note that providing external heating to the system can substantially change the convection patterns. In particular it was revealed that the flow is enhanced when the heating element lies below the liquid-vapour interface; on the contrary, when the heating element is above the liquid-vapour interface and sufficient power is provided, the flow pattern is reversed with respect to the unheated situation. This important result confirms the fact that the phenomena being studied here are strongly dominated by the action of surface tension, because of the strong link between surface tension and temperature.

The second part of the paper reports for the first time on the appearance of thermal instabilities in the evaporation of Methanol, Ethanol & FC72 droplets. The appearance of wave-like thermal fluctuations is clearly observed for both Methanol and Ethanol, and the similarities between these waves and the HTW reported in literature are investigated. FC72 is also found to exhibit thermal fluctuation; however these take the form of thermal cells which propagate radially from the drop centre to the periphery. By investigating the observed behaviour a greater insight into the underlying process is sought.

REFERENCES

[1] Bénard, H., *Rev. Gén. Sci. Pures Appl.*, Vol. 11, 1900, pp. 1261-1309

[2] Bénard, H., *Ann. Chem. Phys.*, Vol. 23, 1901, pp. 62

[3] Levich, V. G., Krylov, V. S., Surface tension driven phenomena, *Annu. Rev. Fluid Mech.*, Vol. 1, 1969, pp. 293-316

[4] Pearson, J. R. A., On convection cells induced by surface tension, *Journal of Fluid Mechanics*, Vol. 4, 1958, pp. 489-500

[5] Scriven, L. E. and Sternling, C. V., The Marangoni effects, *Nature* Vol. 187, 16 July 1960, pp. 186-188

[6] Maidanik Y., Solodovnik N. and Fershtater Y., Investigation on dynamic and stationary characteristics of a loop heat pipe, *9th International Heat Pipe Conference*, Albuquerque, NM., 1995

[7] Dickey J. T. and Peterson G. P., Experimental and analytical investigation of a capillary pumped loop, *Journal of Thermophysics and Heat Transfer*, Vo. 8, 1994, pp. 602-607

[8] Pratt D., Hallinan KP., Thermocapillary Effects on the Wetting Characteristics of a Heated Curved Meniscus, *Journal of Thermophysics and Heat Transfer*, Vol. 11, 1997, pp. 519-525

[9] Kim I., P Wayner, Shape of an evaporating completely wetting extended meniscus, *Journal of Thermophysics and Heat Transfer*, Vol.10, pp. 320-325

[10] Höhmann C., Stephan P., Microscale temperature measurement at an evaporating liquid meniscus, *Experimental Thermal and Fluid Science*, Vol.26, 2002, pp.157-162

[11] Swanson L., Herdt G., Model of the Evaporating Meniscus in a Capillary Tube. *Journal of Heat Transfer*, Vol. 114, 1992, pp. 434-441

[12] Pratt D., Brown J., Hallinan K.P., Thermocapillary Effects on the Stability of a Heated, Curved Meniscus, *Journal of Heat Transfer*, Vol. 120, 1998, pp.220-226.

[13] Buffone C., Sefiane K. and Christy J.R.E., Micro-PIV investigation of thermocapillary Marangoni convection for an evaporating meniscus, *Experiment in Fluids*, Article to appear, 2004

[14] Buffone C., Sefiane K., Christy J.R.E., Experimental investigation of the hydrodynamics and stability of an evaporating wetting film placed in a temperature gradient, *Applied Thermal Engineering*, Vol. 24, 2004, pp.1157-1170

[15] Davis S.H., Annual Review of Fluid Mechanics, Vol.19, 1987, pp.403–435

[16] Smith, Marc K., Stephen H. Davis, *J. of Fluid Mechanics*, Vol. 132, 1983, pp. 119–144

[17] Smith, M. K., *Physics of Fluids*, Vol.29, 1986, pp. 3182

[18] Schwabe D., Möller U., Schneider J. and Scharmann A., *Physics of Fluids*, 1992, pp. 2368–81

[19] Riley R.J., Neitzel G.P., *J. Fluid Mech*., Vol. 359, 1998, pp. 143-164

[20] Garnier N. and Chiffaudel A., *Eur. Phys. J. B*, Vol. 19, 2001, pp. 87–95

[21] Schwabe D., Zebib A., Sim B.C., *J. Fluid Mech*., Vol. 491, 2003, pp. 239-258

[22] Ward C.A., Duan F., *Physical Review E*, Vol. 69, 2004

[23] Ristenpart W.D., Kim P.G., Domingues C., Wan J., Stone H. A., *Phys. Rev. Letters*, Vol. 99, 234502, 2007

[24] Hu H., Larson R.A., Langmuir, Vol. 21, 2005, pp. 3972-3980

[25] Markus R., Willert C., Kompenhans J, Particle Image Velocimetry: a practical guide. Springer, London, 1998

[26] Newport N., Curtin D., Davies M., A comparison of Micro-PIV experiments in a mini-channel to numerical and analytical solutions, *1st Int. Conf. Micro- Minichannels*, Rochester, NY, USA, 2003

[27] Santiago J.G., Wereley C.D., Meinhart C.D., Beebe J.D., Adrian R.J., A particle image velocimetry system for microfluids. Exp. Fluids, Vol. 25, 1998, pp. 316-319

[28] Meinhart C.D., Wereley C.D., Santiago J.G., PIV measurements of a microchannel flow, *Exp. Fluids 27*, 1999, pp. 414-419

[29] Buffone C. and Sefiane K., Investigation of thermocapillary convective patterns and their role in the enhancement of evaporation from pores, *International Journal of Multiphase Flow*, Vol. 30, pp. 1071-1091, 2004

[30] Buffone, C. and Sefiane, K., IR measurements of interfacial temperature during phase change in a confined environment, Vol. 29, pp. 65-74, 2004

[31] Buffone, C. and Sefiane, K., Easson W., Marangoni-driven instabilities of an evaporating liquid-vapor interface , *Physical review E*, Vol. 71, 056302, 2005.

[32] Mancini H., Maza D., *Europhysics Letters*, Vol. 66 , 2004, pp. 812–818